

Impact of Colony Morphologies and Disinfection on Biological Clogging in Porous Media

HUBERT J. DUPIN AND
PERRY L. MCCARTY*

*Department of Civil and Environmental Engineering,
Stanford University, Stanford, California 94305-4020*

Biological clogging of aquifers and other porous media during bioremediation, sand filtration, and aquifer recharge is a significant problem that is yet poorly understood and controlled. One major difficulty is the relatively few direct observations of clogging phenomena, which are required to adequately validate numerical models for predicting flow through porous media. Visualization of biological growth with time and accompanying reductions in hydraulic conductivity were obtained using two-dimensional micromodels of porous media. The micromodels were seeded with mixed microbial cultures to allow natural selection of dominant aerobic morphologies following continuous feed of culture media containing 1.36–1.69 mM acetate flowing at 0.9–3.6 m/day specific discharge velocity. Of the several different resulting colony morphologies, filaments dominated at pH 3, while biofilms and aggregates dominated at neutral pH. Conductivity decrease correlated with biological growth and morphology, and sudden conductivity recoveries correlated with sloughing events. Periodic chlorine disinfection resulted in temporary increase in conductivity and helped open channels of flow between dense colonies. However, aggregates of organisms exhibited increased resistance to chlorine disinfection with time, reducing disinfection effectiveness. Continuous, rather than periodic, disinfection is recommended. Models for biological substrate removal and clogging should incorporate different growth morphologies to produce satisfactory simulation results.

Introduction

Bioremediation is potentially a cost-effective method to restore in-situ contaminated aquifers (1). Several factors impact the total cost. While biological parameters, such as growth-substrate requirements and degradation rates, play a significant role, particularly in the case of cometabolism (2), greater costs may be associated with clogging of the aquifer (e.g. energy for pumping) or costs associated with prevention of clogging (e.g. well redevelopment and disinfection) (3). Thus, cost optimization of a bioremediation scheme requires a good understanding of the processes of biological growth in porous media and their control.

Studies on biological growth in porous media have mainly focused on wastewater treatment units; the principal interest of such investigations has been optimizing degradation rates and substrate loading, whereas clogging has not been studied as thoroughly. Biological growth is usually modeled as a uniform coverage of support media by microorganisms, i.e. biofilms (4–7). By analogy, biological growth in fine grained

porous media has mainly been modeled as biofilms (8–12) or as coverage by microcolonies, i.e. patchy biofilms (13).

Rittmann (14) observed that continuous biofilms can be sustained with high loadings but that patchy growth is more likely at lower loadings. He further added that the distinction between continuous and patchy biofilm is not crucial to model substrate removal but may be important to model clogging (14). Indeed, Vandevivere et al. (9) observed that biofilm models do not reproduce permeability reduction measured in porous media with grain sizes smaller than a millimeter, grain sizes relevant to in-situ bioremediation, whereas assuming aggregate growth could lead to realistic permeability reduction, i.e., greater permeability reduction than biofilms for the same total amount of biomass. Thus, it is believed that biological growth morphologies and their interactions need to be better understood, that is observed, before accurate modeling of clogging in fine grained media can be undertaken.

Few investigators have focused on observing biological growth morphologies in porous media mimicking fine sand, that is, with grain sizes smaller than a millimeter. Vandevivere and Baveye (15) observed aggregate formation using a pure culture of *Arthrobacter* sp. They also investigated clogging effects using other pure cultures with different behaviors (16). Similarly, Taylor and Jaffe (17) investigated clogging effects of mixed cultures derived from activated sludge. Paulsen et al. (18) observed biological growth of seawater microorganisms in micromodels supplied with a medium containing oil droplets. Nevertheless, actual observations of biomass growth and clogging in porous media relevant to bioremediation conditions are sparse in the literature. Most observations have been made at the end of an experiment by dismantling the porous media, which does not provide good understanding of the dynamics of biological growth at the microscale. The factors important in biological clogging, however, are well-known and have been comprehensively reviewed by Baveye et al. (19).

Several investigators have addressed the effects of disinfection on biological clogging in aquifers. With studies on groundwater recharge, Ehrlich et al. (20) and Vecchioli et al. (21) showed that maintaining a residual chlorine concentration greater than 2–2.5 mg/L reduced clogging in general and in some instances prevented clogging by microorganisms. McCarty et al. (3) used hydrogen peroxide to control biological clogging near the injection well during in-situ bioremediation. They showed that continuously amending the feed solution with a low hydrogen peroxide concentration (47 mg/L) prevented excessive clogging, whereas intermittent disinfection with higher concentrations (71 mg/L) had only a temporary beneficial effect. However, the pore scale efficiency or dynamics of such disinfection schemes has not been widely investigated.

To develop a better understanding of the dynamics of biological growth and disinfection, we have developed an apparatus (22) that allows both spatial and temporal observations of two-dimensional micromodels, that is both at the microscale (size of a pore, 500 μ m) and mesoscale (size of a micromodel, cm) and using both short time-lapse observations (up to 20 images/s for a single pore) or long time-lapse observations (complete scanning of the micromodel every 4 h). This paper compiles observations of biological growth and clogging in three micromodels, called Silicon Pore Imaging Elements (SPIEs), seeded with mixed cultures, grown on acetate, and exposed at times to chlorine for disinfection.

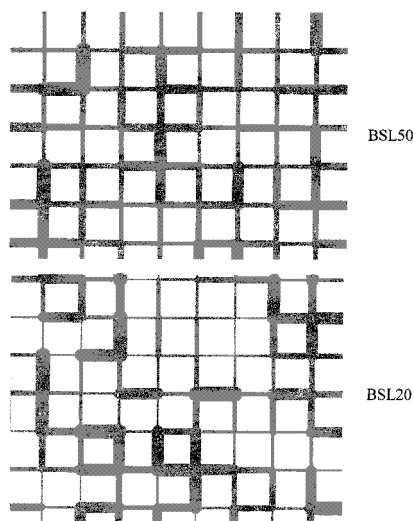


FIGURE 1. Illustration of a 3.2 mm \times 4.3 mm area of the two SPIE patterns.

A mixed culture rather than pure cultures was used to better mimic growth of indigenous microorganisms that are likely to be present at a typical in-situ bioremediation site. Indeed, the experiments reported here showed occurrence of several simultaneous forms of growth following acetate feeding. This paper focuses on the observation of the simultaneous diversity and interactions of the different colony morphologies under different environmental conditions, with the goal of formulating novel assumptions for proper modeling of biological growth and clogging in fine grained porous media.

Material and Methods

Details of SPIE manufacture, operation, and image analysis procedures were described previously (22).

SPIE Construction. In summary, networks of interconnected channels (ball-and-stick model) with overall dimensions of 13.5 mm \times 28 mm were etched 200 μ m deep into silicon wafers. Two different channel width distributions were used. In the first pattern, called BSL50, channel widths were randomly drawn from a log-normal distribution (mean 75 μ m, standard deviation 47 μ m, lower and upper cutoff sizes 50 μ m and 200 μ m, respectively). In the second pattern, called BSL20, channel widths were randomly drawn from a log-normal distribution (mean 123 μ m, standard deviation 204 μ m, lower and upper cutoff sizes 20 μ m and 200 μ m, respectively). The nodes, spaced 500 μ m apart on a 27 \times 57 square grid, were circular with a diameter equaling the maximum of the widths of the incoming channels. These networks simulate the random pore spaces in fine homogeneous sands, BSL20 being less homogeneous than BSL50 (Figure 1). The porosity was 37% and 32% for BSL50 and BSL20, respectively, and the void volume was 28 and 24 mm³, respectively, based on an etching depth of 200 μ m.

Image Acquisition and Analysis. Each SPIE was mounted in a machined holder to which the fluid lines were connected. This holder was fastened on the motorized stage of an inverted microscope (22). The SPIE was completely scanned every 4–6 h, each scan requiring the acquisition of 1600–1800 images. At each stop, an image was acquired in bright field microscopy that represented a 685 μ m \times 480 μ m portion of the SPIE. These individual images were concatenated into a meso-image. A series of filters was applied to the meso-images to detect and enhance viewing of biological growth. Because images were focused at mid-thickness of the SPIEs, only microorganisms that developed out in the pore space were focused. Polymer foot prints with sorbed material would appear blurred.

SPIE Operation. The hydraulic head across the SPIE was measured using a Validyne suite (www.validyne.com) consisting of a DP105 pressure transducer equipped with a 3–20 diaphragm and connected to a CD379 Portable Carrier Demodulator. The 5–20 mA current signal was acquired by measuring the voltage across a 250 Ω resistor placed in series on the 12V power source, using a National Instruments PC-LPM-16\ PnP board (www.natinst.com) and a custom-written software program.

Two BSL20 SPIEs were initially disinfected by flowing through them a diluted solution of hypochlorite (12.5–50 mg/L as chlorine), neutralized with a sterile sodium sulfite solution, and then rinsed with sterile demineralized water. The BSL50 SPIE was disinfected with a 10% nitric acid solution and rinsed with sterile demineralized water (22). However, rinsing of this BSL50 SPIE was somehow incomplete and the resulting pH of the effluent throughout the whole experiment remained about 3, while it was between 6.8 and 7.2 for the two BSL20 experiments. Settled influent municipal wastewater from the Palo Alto Wastewater Treatment Plant, incubated aerobically for about 20 h in a solution containing about 1.36–1.69 mM acetate (80–100 mg/L as acetate), was diluted 1:10 in demineralized water immediately prior to being used to seed the SPIEs similarly to the procedure used previously (22).

The feed solution contained about 0.34–0.5 mM acetate (20–30 mg/L as acetate) in a mineral salt solution similar to that of BOD dilution water (23), but with twice the amount of ammonium chloride to provide enough nitrogen for biological growth. Cotton sterile filtered oxygen was bubbled through the solution while stirring vigorously. This solution was syringe-pumped into the SPIEs at various flow rates. The resulting specific discharge was 0.9–3.6 m/day, and the average interstitial velocity, accounting for porosity of clean SPIEs, was between 2.4 and 11.2 m/day. This represents the relatively high velocities that could prevail during enhanced bioremediation, filtration, or groundwater recharge.

Flow rate or head across the SPIEs was quadrupled for 5–15 min at different moments (see below) to produce significant sloughing within the SPIE. These events were called “redevelopment”, by analogy to the restoration of hydraulic conductivity during in-situ bioremediation.

In the case of the low pH SPIE, a commercial grade bleach solution (Clorox) was diluted 1:10 000 in demineralized water for use as a disinfectant and was fed for 6 h, 4 days after inoculation. The residual chlorine concentration of the diluted solution was measured as 5 mg/L by the starch iodide method (23). In the case of a BSL20 SPIE, Clorox was diluted 1:1250 in the oxygenated feed solution, yielding a chlorine concentration of 40 mg/L and an acetate concentration of 0.34 mM. This solution was fed during 8, 12, or 14 h at about 5 day intervals, preceded or not by redevelopment (see below). After each disinfection, normal feed was restored. The chlorine concentration for the low pH SPIE was chosen much lower than the one for neutral pH SPIE: being fed for less time before disinfection, its chlorine demand was likely lower. While relatively high, these chlorine concentrations are significantly lower than concentrations used by Ehrlich et al. (20) and Vecchioli et al. (21) for groundwater recharge studies.

Results

SPIE observations can provide precise quantitative results when using pure cultures or man-made mixed cultures because the colony morphologies are known a priori. However, when using “natural” mixed cultures, colony morphologies are an output of the system. Distinction between the different observed morphologies cannot be drawn clearly (see below) particularly if they slowly evolve from one type, e.g. aggregates, to uniform coverage (biofilm).

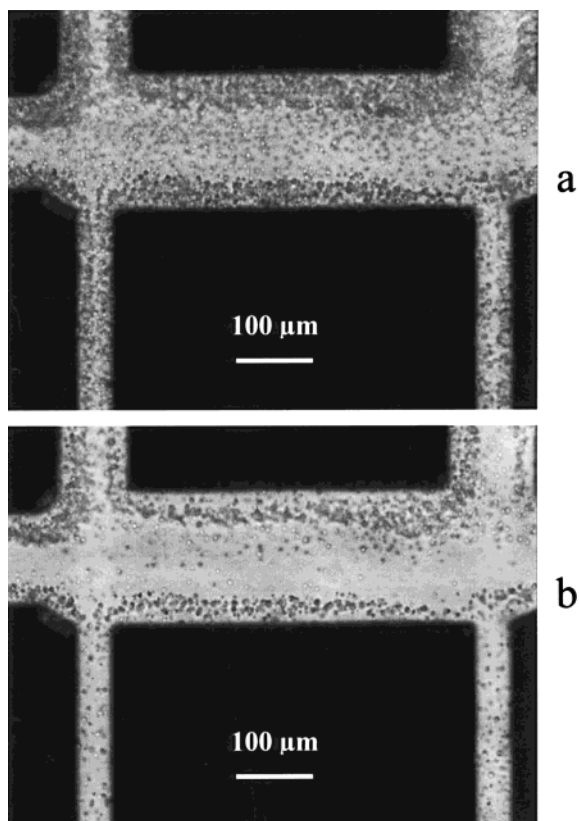


FIGURE 2. Forty to $60\ \mu\text{m}$ thick biofilm developing at the upgradient end of a BSL20 SPIE after 2 weeks of acetate feeding. Thickness can be measured from the denser growth visible on the sidewalls in this top view. The lower picture was acquired 4 h later and shows evidence of sloughing.

Thus, accurate quantitative analysis of results in terms of frequency of different types of colony morphologies, growth rates, or efficiency of disinfection was unfortunately not feasible. However, colony dynamics and interactions were purposely observed through comparison of many time-lapse movies of adjacent pores and the whole SPIEs. In a sense, this paper summarizes observations of about 500 000 pore images of biological growth.

Each SPIE realization is unique because results are contingent upon what kinds of organisms attach and where they attach. When using natural mixed cultures and considering mesoscale colony shape, cross-SPIE reproducibility was not possible to achieve. However, what is reproducible are the local phenomenon that result in space colonization, for example. Thus, reproducibility of the observations is ensured by the spatial and temporal repetition of local phenomenon within a given SPIE. For example, reproducibility of disinfection effects with the BSL20 SPIEs was ensured by a triplicate sequential experiment on the same SPIE.

In all of the figures, regional (Darcy) flow is from left (upgradient) to right (downgradient).

Colony Morphology. As expected, a uniform coverage of the SPIE surface with a biofilm up to $60\ \mu\text{m}$ thick developed in the BSL20 SPIEs (Figure 2). Sloughing of biofilms in pores was frequently observed, both in space and in time (once every few days in many channels). In addition, aggregates grew in some channels (Figure 3). Within 5–10 days, aggregates spanned across $200\ \mu\text{m}$ wide channels or in some cases across $50\ \mu\text{m}$ wide channels in a day. In some channels, the resulting colonies showed features of both biofilms and aggregates, that is they were thick, dense, and covered only part of the surface as aggregates but were wide and shallow as biofilms. In such cases, a distinction between a biofilm or

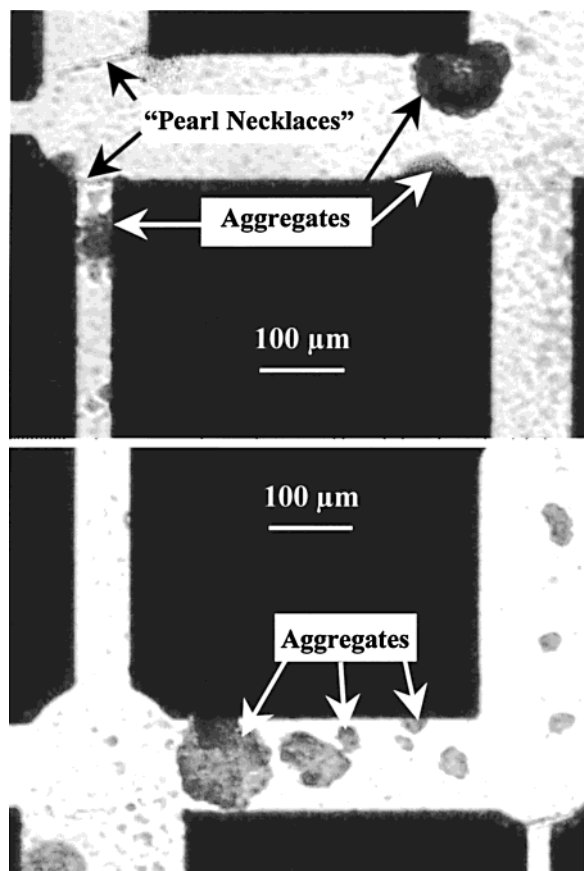


FIGURE 3. Biological growth morphologies following 10 days of acetate feeding to a BSL20 SPIE included different types of aggregates and strings. The fuzzy background is due to thin biofilm growth on the top and bottom plates.

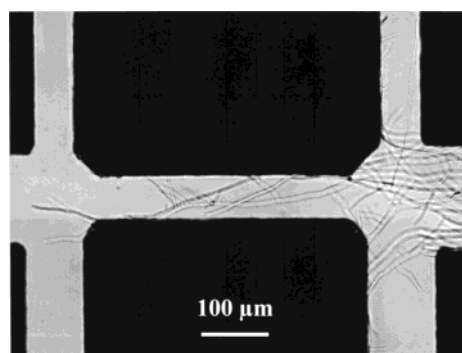


FIGURE 4. Filamentous growth in a BSL50 SPIE.

an aggregate morphology was difficult to draw. This particular reason exemplifies the difficulty of accurate quantitative analysis.

Spanning across the junctions of channels of the BSL20 SPIEs, straight strings ($2\text{--}3\ \mu\text{m}$ wide, up to $200\ \mu\text{m}$ long) were frequently observed, on which cells seemed to attach, in a pearl necklace fashion (Figure 3). The nature of such filaments is unknown. In some instances, aggregates formed on the strings or used the strings as a support to grow out into the channels. It is very likely that these aggregates had a higher exposure area to substrate than aggregates growing on pore walls and thus would less likely be mass transfer limited.

As described previously (22), filamentous growth (Figure 4) dominated under acidic conditions. After only about 4 days, growth of 12 initial colonies resulted in colonization of a significant portion of the BSL50 SPIE. From culturing of

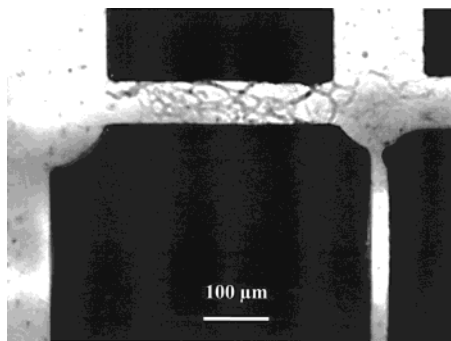


FIGURE 5. Bioweb in a pore of a BSL20 SPIE.

spores in the effluent, it was presumed these spore-forming filaments were *Acremonium* sp. fungi. Filamentous growth was also observed frequently at neutral pH, but colonies remained smaller than a millimeter, that is more than 100 times smaller in surface than in the low pH SPIE.

In one of the BSL20 experiment, motile cells, swimming at velocities of about $100 \mu\text{m/s}$, were observed initially throughout the SPIE. Whereas these cells could readily progress in any direction in some channels, they were flushed downgradient in the center of channels with high velocity but were also observed to progress slowly upgradient in the same channels by swimming close to the pore walls.

Finally, a bioweb (Figure 5) developed in some channels of a BSL20 SPIE. This form of growth consists of interlaced strings ($3\text{--}7 \mu\text{m}$ wide). A similar form was reported by Paulsen et al. (18). These strings grew in length and width with time and appeared very different from the above-mentioned straight strings (“pearl necklaces”). It is likely that this form of biological growth facilitates substrate mass transfer compared to biofilms.

Colony Dynamics. SPIE observations over both time and space provided insights into both biofilm dynamics and the validity of assumptions regarding modeling of biological growth in porous media. In both BSL20 experiments, a biofilm developed initially throughout the entire SPIE, with aggregates localized only in a few places. After 12 days, however, continued aggregate and biofilm growth was readily visible only at the upgradient end of the SPIEs, while downgradient aggregates and biofilm no longer expanded noticeably, likely because of starvation due to substrate absence, confirmed by analysis for acetate in the effluent. Thus, growth occurred mainly over a few millimeters at the upgradient portion of the SPIE, as noted previously with filamentous growth (22), instead of over the centimeter scale commonly measured by others (15, 17). Interestingly, this happened even with average interstitial velocities of about 10 m/day .

Step-increases in flow rates through the SPIE revealed significant biofilm dynamics. Upgradient biofilms generally did not thicken noticeably. Rather, they often seemed to become thinner with time, in apparent contradiction with an expected thickening because of increased mass transfer but consistent with the effect of detachment on the control of biofilm thickness. This phenomenon is confirmed by the development of a similarly thick biofilm slightly downgradient in the SPIE, suggesting that substrate was still readily available at these downgradient locations.

The different growth morphologies appeared to resist shear stresses differently. Sometimes, narrow channels appeared devoid of any growth, although their adjacent upgradient and downgradient channels were colonized by a biofilm. When aggregates developed in one of these initially empty channels and reached the opposing wall, biofilm-forming organisms immediately colonized the channel. From the mesoscale inspection of the SPIE, such narrow channels appeared to be the bottlenecks of mesoscale flowpaths, where

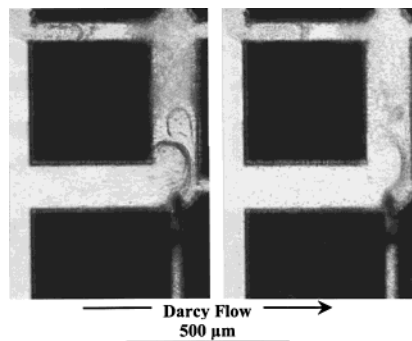


FIGURE 6. Breaking of an upgradient dam and downstream sloughing in a BSL20 SPIE. Right image was acquired 30 h after left image.

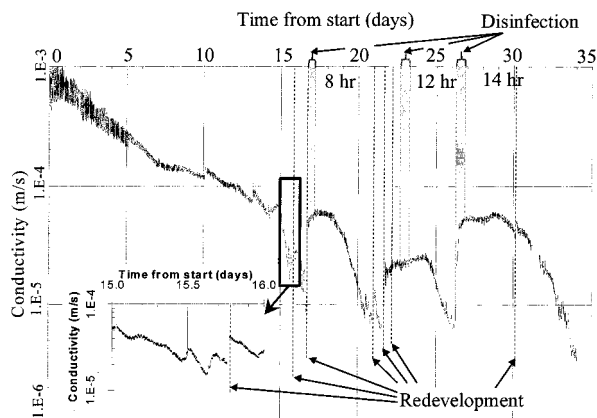


FIGURE 7. Hydraulic conductivity measurements as a function of time for a BSL20 experiment. Because of pressure transducer limitations, minimum measured conductivity was $6.4 \times 10^{-6} \text{ m/s}$ until day 33.5. The insert shows how sloughing resulted in sudden conductivity recoveries between day 15 and 16.

fluid velocities, hence shear stresses, would be expected to be high. In other instances, some thick biological masses seemed at times to form plugs in channels. When one of these plugs detached, significant sloughing of the downgradient biofilm was observed (Figure 6). These observations suggest that such plugs created dams, shielding less resistant downgradient colonies from excessive shear stresses.

Figure 7 shows the evolution with time of the average hydraulic conductivity of a BSL20 SPIE, computed as $k = QL/WT\Delta\phi$, where Q is the flow rate through the SPIE; L , W , and T the length, width, and thickness, respectively, of the SPIE; and $\Delta\phi$ the head loss monitored across the SPIE. During the first 2 weeks of the experiment, conductivity slowly and regularly decreased as biomass colonized the SPIE. Thereafter, when the upgradient part of the SPIE became dense with biomass, conductivity rapidly decreased. Sudden permeability recoveries were correlated with sloughing events that occurred in adjacent channels delineating mesoscale flow paths. This overall behavior can be explained by percolation theory as the SPIE reached the percolation threshold (24, 25). Because of heterogeneity of channel conductivity, water would flow mainly through preferential pathways; conductivity would slowly decrease with porosity reduction until the clogging of a preferential pathway caused permeability to suddenly drop. Whenever sloughing occurred along a preferential pathway, this pathway would then conduct again significant flow, and permeability would suddenly increase, as observed. Nonetheless, the overall effect was clogging, the final conductivity being reduced by a factor of about 200 compared to the initial one.

“Redevelopment” caused a partial recovery in conductivity as shown in Figure 7. However, such recovery was only

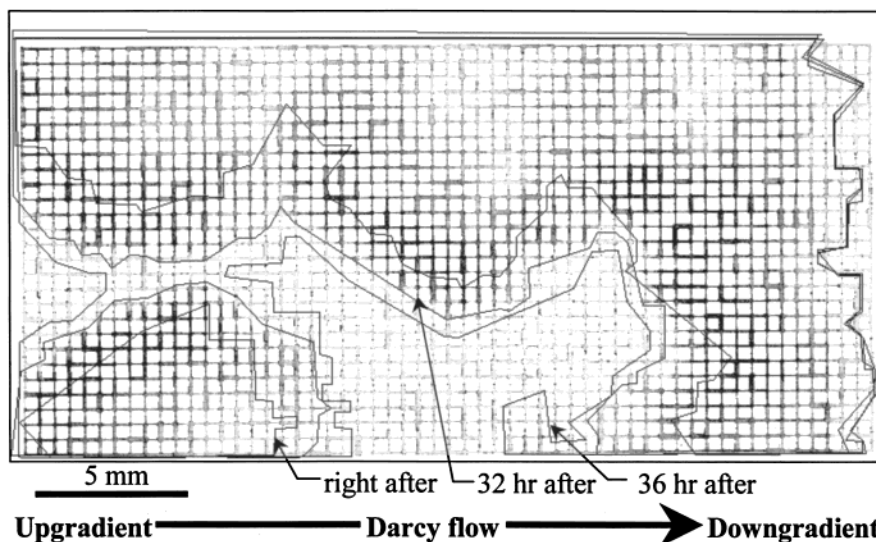


FIGURE 8. Comparison of mesoscale biofilm outline right after disinfection was stopped with that resulting 32 and 36 h after acetate feed was restored to a BSL50 SPIE. The overlays show the increased extent of biofilm growth resulting from the restored acetate feed.

temporary; it took less than a day for the conductivity to drop below its level before redevelopment.

Effect of Disinfection. Disinfection at low chlorine concentration induced different effects within the low pH SPIE where initial filamentous growth had filled a large portion of the channels of the SPIE (Figure 8) (22). Some filamentous colonies, whose lengths were on the order of a pore length, detached. However, no major detachment of the larger filamentous colonies was observed. Rather, the outer portion of the colonies in contact with the open channel stopped growing, as would be expected since acetate feeding was stopped. In some instances, the exposed ends of the filaments retracted and folded onto themselves, suggesting an impact from the disinfectant. In portions of the dense colonies, generally away from the open channel, some filaments continued to grow during disinfection at a very low rate. Such continued growth may have resulted from diffusion and/or advection of residual acetate into the colonies, absence of residual acetate transport out of the colonies, or consumption of internal reserves by the filaments. Interestingly, if we consider that the intermingled filamentous colonies throughout the SPIE in Figure 8 resulting from the initial acetate feeding formed a mesoscale biofilm, the thickness of that biofilm would be about 1 cm. Given a typical aqueous diffusion coefficient of $1 \text{ cm}^2/\text{d}$, the 6 h disinfection time used would be shorter than the characteristic time for chlorine to diffuse the 1 cm distance into the biofilm in the absence of reaction. Given that hypochlorite is a reacting solute, the characteristic time to move 1 cm would be even longer. The same reasoning applies to acetate, so that the outer portions of the colonies could starve and stop growing, while acetate could still be available within the inner portions of the colonies during disinfection.

When acetate feed was restored, growth did not result from the terminal ends of the filaments at the outer portion of the colonies where the most active growth had resulted previously. Rather, new filaments emerged from deeper within the dense colonies, their rapid growth resulting in the closing of the open channel within 36 h (Figure 8). Based upon the microscale and mesoscale measured growth rates of 1.5 and $1.1 \mu\text{m}/\text{min}$ in the upgradient and lateral directions, respectively, prior to disinfection (22), unharmed filaments would grow an estimated 2.9 and 2.1 mm, respectively, in 32 h. These lengths represent about four to six "grains" in the SPIE, about the distance the leading edge of the colonies moved following disinfection (Figure 8). Thus, the filaments

must have resumed growth following disinfection almost from their extremities near the open channel. Direct observation of the exact location where growth resumed was not possible because of the high filament density present. Disinfection appeared therefore to harm only the very outermost portion of the filaments.

In the other disinfection experiment, biomass growth had resulted in a thick biofilm completely colonizing the entire upgradient end of a BSL20 SPIE after 16.5 days of initial acetate feed at increasing flow rates, up to 0.4 mL/h. From then on, flow rates were maintained at 0.2 mL/h, yielding an average velocity of about 5.2 m/day in a clean BSL20 SPIE. Normal feed was then replaced with chlorinated feed for an 8–14 h period about every 5 days, and chlorination was sometimes preceded by hydraulic shocks (Figure 7).

Whereas an open flow channel preexisted before disinfection in the low pH SPIE in the case of filamentous growth, no mesoscale open flow channel was apparent in the BSL20 SPIE before disinfection began as a thicker biofilm had colonized uniformly all the pores on the upgradient end of the SPIE. However, during each chlorination event, biofilm sloughing resulted in the opening of a few mesoscale flow channels in the middle to lower portion on the upgradient side of the SPIE (Figure 9). As chlorination continued, the opened channels became wider. However, despite the high chlorine concentration used (40 mg/L) and the long exposure time (8–14 h), some biofilm-forming microorganisms survived disinfection in the 2–8 mm wide remaining biomass areas (shown as dark channels in Figure 9). With time, an increasing number of dense colonies formed downgradient (shown as black squares in Figure 9). Soon after chlorination was stopped, microorganisms rapidly recolonized the SPIE. Thus, chlorination appeared qualitatively to have only eroded the outer layers of the separated mesoscale colonies similarly to the filamentous growth case. Since only the outermost edges of the colonies appeared harmed by disinfection, chlorine consumption by biomass may have been greater than the hypochlorite supply. High chlorine consumption is also suggested by the temporary absence of sloughing or other adverse effect of disinfection directly downgradient of a channel once opened by disinfection.

Unexpectedly, the front end of the large remaining biomass areas was not completely eroded by disinfection (Figure 10). Careful observation of microscale images revealed that some thick and dense biological masses remained after disinfection and subsequent biofilm sloughing. This suggests

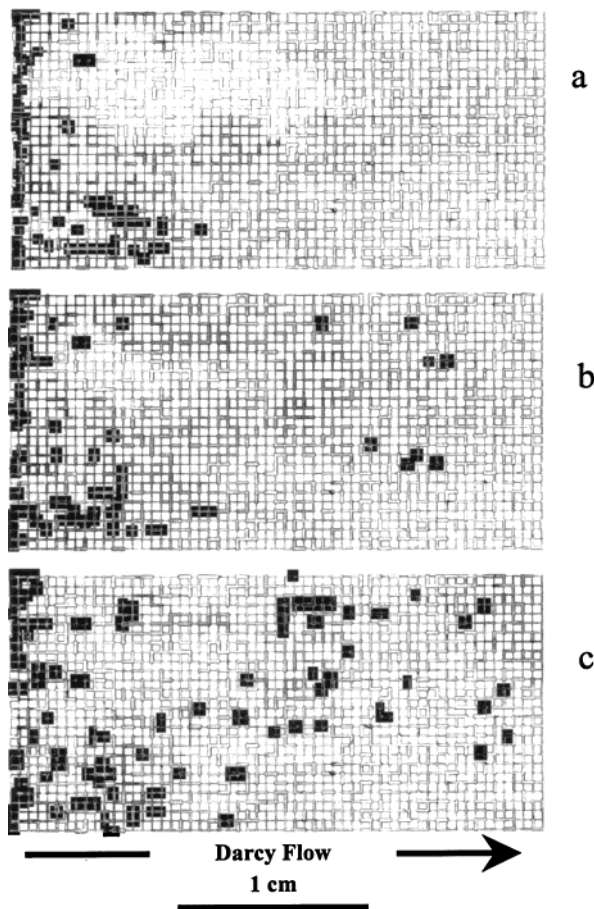


FIGURE 9. Effect of disinfection and subsequent feeding on colony growth in a BSL20 SPIE. The dark areas show locations of strongly attaching and dense biological growth. These meso-scale images were acquired just after disinfection (a, day 16; b, day 22; and c, day 26). The top meso-image shows a clear open flow path.

either that hypochlorite was forced around the less conducting areas, shielding some downgradient portions of the SPIE from disinfection, or that hypochlorite was consumed by contact with these barriers so that a chlorine free medium flew through them. This could explain the opening of flow channels between the resistant upgradient barriers and the slow erosion of the side and back of the mesoscale colonies, as diffusion would there be the main chlorine transport phenomenon.

Shortly before the first two chlorinations, hydraulic shocks were performed, and conductivity then sharply increased (Figure 7). These shocks may have helped create the open flow channel through which chlorinated feed could readily flow. During chlorination, hydraulic conductivity increased somewhat, which is correlated with the slow erosion of the mesoscale colonies. Following disinfection, hydraulic conductivity remained constant for 1–2 days and then decreased sharply, longer lag-times corresponding to longer disinfection events. No hydraulic shock was made before the third chlorination, and conductivity initially increased rapidly, but slower than from hydraulic shocks, suggesting a strong and rapid impact of disinfection.

The third chlorination was sufficiently long to remove almost all of the observable biological mass throughout the SPIE (Figure 9), except some biological mass identified previously as strongly attaching in pre-disinfection observations (Figure 10). Yet, conductivity was then about 12–16 times lower than the initial conductivity of a clean SPIE. This suggests that these stronger attaching biological masses were largely responsible for the major conductivity decrease.

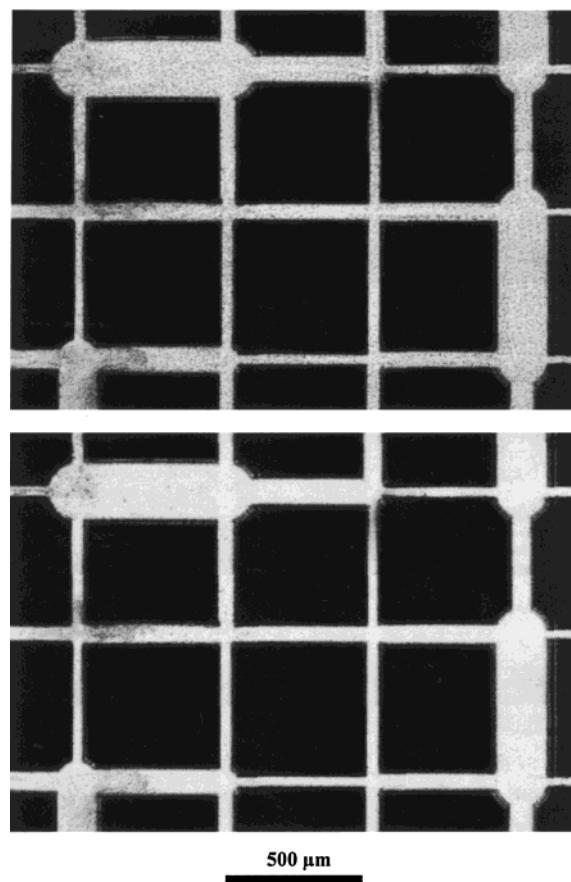


FIGURE 10. Effect of disinfection on biofilm covered BSL20 SPIE. The top picture was acquired right before the third disinfection event; the bottom picture, acquired 16 h later, shows biofilm sloughing had resulted, but stronger attaching organisms remained in some of the left-most channels.

Discussion

SPIE observations bear several implications to modeling of biomass growth in porous media, in terms of substrate consumption, permeability decrease, and resistance to disinfection.

A biofilm is the most commonly modeled form of growth. Because of the large surface area of porous media, a thin biofilm can occupy a significant volume, thus effecting rapid substrate removal and growth as noted at the upgradient end of the SPIE. However, Vandevivere et al. (9) showed that permeability predictions based on porosity reduction by biofilms alone underestimate observed permeability reductions. Figure 11 shows numerical simulations obtained using network models and assuming that biological growth occurs only as aggregates that are almost impermeable to flow (details of this model are given by Dupin (26)). Aggregate growth induces a much greater permeability reduction for a given porosity reduction than biofilm based models, that is, closer to what is often observed (15, 17, 27). However, aggregates are more compact than biofilms, and mass transfer, hence substrate degradation, is likely to be smaller for aggregates than for biofilms for a given porosity reduction. Thus, assuming the sole presence of aggregates is likely to result in better predictions of permeability reduction but an underestimation of substrate consumption.

Different culture morphologies were found here to resist shear stresses to different extents. Similarly, it is very likely that different microorganisms growing with the same morphologies would resist shear stresses differently. In the case of biofilm growth, much sloughing occurred during disinfection.

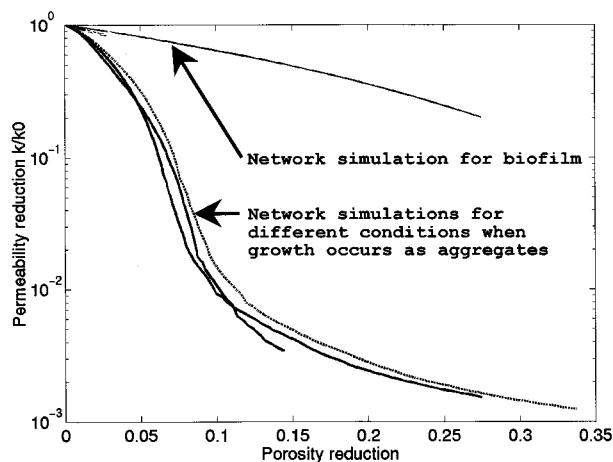


FIGURE 11. Relative hydraulic conductivity $k(t)/k(t=0)$ as a function of porosity reduction for different network realizations and different parameter values. Aggregates resist to flow so that a 100% porosity reduction would yield a reduction of permeability of the network by 2000. The "biofilm curve" is achieved by redistributing as an impermeable layer on the pore walls the volume of the aggregates computed for one of the aggregate simulations.

tion, but many strongly attaching biological masses remained. In the case of filamentous growth, small colonies detached, while the colonies whose long filaments were woven between the SPIEs grains remained even during disinfection. Such woven colonies would likely need to be broken into tiny fragments before migrating through porous media, which would likely require exceptionally high shear stresses. These observations suggest that weakly attaching organisms are likely to be washed out, while the stronger attaching organisms are likely to persist: selection might lead to greater number of strongly attaching organisms, as was observed during the 3-week course of the BSL20 experiment (Figure 9). Because the macroscopic energy needed for pumping (product of the flow rate and the head loss) results from the energy dissipation by viscous forces at the microscale, that is shear stresses, resistance to higher shear stresses could result in greater head losses, greater pumping expenses for the same pumping flow rate, and greater permeability reductions, everything else being kept identical (colony morphology and porosity reduction). Microorganisms that attach strongly to the surface and to each other are likely to be the most effective at reducing permeability.

As found here, different morphologies may occur at the same time. This yields locally to a different relation between porosity reduction, that is biomass, and permeability reduction. Upscaling of porosity-permeability relations from different local biological clogging behaviors would depend on the relative abundance of different microorganism morphologies, which might be given only by a detailed pore scale model.

Of importance also were the observations of filamentous growth. The filamentous organisms appeared to orient themselves by chemotropism or rheotropism (22), mechanical stress, or flow sensing behaviors widely described in the fungi literature (28). We did not observe any detachment of filaments, neither during growth nor during disinfection. Thus, a reasonable modeling assumption for fungal growth would be to neglect detachment, except at early stages of growth when filaments are small enough to flow in one piece or very close to an injection well where velocities, and hence shear stresses, are highest.

Other forms of growth need to be addressed experimentally before being modeled. In particular, some strains are both motile and capable of attachment to surfaces. For example, *Pseudomonas* sp. strain KC has been shown to

migrate toward nitrate by chemotaxis but can also grow on surfaces by Witt et al. (29). They suggested such behavior is likely to enhance colonization throughout the porous media. While it is unclear whether and how motile cells affect permeability reduction while swimming, they would lead to permeability reduction when attached to a surface. Clogging potential by other observed forms of biological growth, such as biowebs and pearl necklaces, is unknown but may be significant. Because such structures may act as sieves and filter out naturally occurring particles or detached cell clusters moving with flow, their potential impact on clogging is likely greater than that which might be expected based on shape alone. Not observed here but likely to occur at times is the presence of higher order organisms, such as protozoa, that may graze on bacteria and contribute to permeability recovery.

In the case of biofilm growth, the initial acetate feeding resulted in uniform SPIE colonization. Shock disinfection did open flow channels, but they subsequently closed once acetate feeding was restored. In this case, the closed channels could be reopened by disinfection events. Hydraulic shocks, such as produced in normal well redevelopment, helped to recover conductivity for a short time period here (about a day). More and greater hydraulic shocks might have had larger impact. From microscale images, it appeared that only a few channels were affected by the hydraulic shocks, that is, effects were very local, the cumulative result of which could be measured at the mesoscale by hydraulic gradient decreases, but not readily observed, in contrast to disinfection, which obviously opened wide channels through the SPIE.

With filamentous growth, disinfection for 6 h with 5 mg/L chlorine had little adverse impact on biological growth: no detachment occurred, filamentous growth resumed immediately once acetate feeding was restored, and within 36 h the SPIE became colonized throughout. In the case of biofilm growth, disinfection for up to 14 h with 40 mg/L chlorine resulted in significant detachment of growth and a temporary opening of flow channels, but these closed as well within 5 days of restoration of acetate feed. The inability to kill some of the biofilm colonies with high chlorine doses over long time periods was probably related to two major factors. One is the low flow rate of disinfectant into the depths of some dense biomass caused either by biofilm clogging of channels, by low hydraulic gradients, such as in lateral channels, or by the centimeter size of the colonies themselves requiring a very long time for diffusion. The other is the consumption of chlorine by biomass as the chlorine either flows or diffuses through it. However, a long disinfection time (14 h) was sufficient to remove most of the biomass within the BSL20 SPIE. Thus, the disinfection tests here reported suggest that intermittent disinfection with a few days between each disinfection event would not be sufficient for preventing extreme biological growth during bioremediation with substrate injection as it may kill desired organisms. Indeed, a continuous disinfectant addition was found more efficient for preventing clogging than intermittent disinfection during full-scale bioremediation (3). There, continuous disinfection with hydrogen peroxide not only maintained good hydraulic conductivity as suggested here but also provided needed oxygen further out in the aquifer where needed for biological growth. These results suggest continuous disinfection at moderate concentrations is a better strategy than intermittent disinfection for controlling biological clogging.

Acknowledgments

This research was supported in part by the Office of Research and Development, U.S. Environmental Protection Agency, through the Western Region Hazardous Substance Research

Center under agreement R-815738, and in part by Elf Aquitaine, Inc. This article has not been reviewed by those organizations, and thus no official endorsement should be inferred.

Literature Cited

- (1) Miller, C. T.; Rabideau, A. J.; Mayer, A. S. *Res. J. Water Pollut. Control Fed.* **1991**, *63*, 552–593.
- (2) McCarty, P. L. *Curr. Opin. Biotechnol.* **1993**, *4*, 323–330.
- (3) McCarty, P. L.; Goltz, M. N.; Hopkins, G. D.; Dolan, M. E.; Allan, J. P.; Kawakami, B. T.; Carrothers, T. J. *Environ. Sci. Technol.* **1998**, *32*, 88–100.
- (4) Atkinson, B.; How, S. *Transactions, Institution Chem. Engineers, Great Br.* **1974**, *52*, 260–268.
- (5) Atkinson, B.; Davies, I. *Transactions, Institution Chem. Engineers, Great Br.* **1974**, *52*, 248–259.
- (6) Rittmann, B. E.; McCarty, P. L. *Biotechnol. Bioeng.* **1980**, *22*, 2343–2358.
- (7) Rittmann, B. E.; McCarty, P. L. *Am. Soc. Civil Engineers, J. Environ. Eng. Division* **1981**, *107*, 831–849.
- (8) Taylor, S. W.; Jaffe, P. R. *Water Resour. Res.* **1990**, *26*, 2181–2194.
- (9) Vandevivere, P.; Baveye, P.; Sanchez de Lozada, D.; DeLeo, P. *Water Resour. Res.* **1995**, *31*, 2173–2180.
- (10) Clement, T. P.; Hooker, B. S.; Skeen, R. S. *Ground Water* **1996**, *34*, 934–942.
- (11) Chen, B.; Cunningham, A.; Visser, E. Numerical simulation of biofilm growth in porous media at the microscale. In *Proceedings of the 11th International Conference on Computational Methods in Water Resources*; Cancun, Mexico; Computational Mechanics Publ.: Southampton, England, 1996.
- (12) Suchomel, B. J.; Chen, B. M.; Allen III, M. B. *Transp. Porous Media* **1998**, *30*, 1–23.
- (13) Molz, F. J.; Widdowson, M. A.; Benefield, L. D. *Water Resour. Res. WREAO* **1986**, *22*, 1207–1216.
- (14) Rittmann, B. E. *Water Resour. Res.* **1993**, *29*, 2195–2198.
- (15) Vandevivere, P.; Baveye, P. *Soil Sci. Soc. Am. J.* **1992**, *56*, 1–13.
- (16) Vandevivere, P.; Baveye, P. *Appl. Environ. Microbiol.* **1992**, *58*, 1690–1698.
- (17) Taylor, S. W.; Jaffe, P. R. *Water Resour. Res.* **1990**, *26*, 2153–2159.
- (18) Paulsen, J. E.; Oppen, E.; Bakke, R. *Water Sci. Technol.* **1997**, *36*, 1–9.
- (19) Baveye, P.; Vandevivere, P.; Hoyle, B. L.; DeLeo, P. C.; Sanchez de Lozada, D. *Crit. Rev. Environ. Sci. Technol.* **1998**, *28*, 123–191.
- (20) Ehrlich, G. G.; Ku, H. F. H.; Vecchioli, J.; Ehlke, T. A. Professional Paper 751-E; U.S. Geological Survey: 1980.
- (21) Vecchioli, J.; Ku, H. F. H.; Sulam, D. J. Professional Paper 751-F; U.S. Geological Survey: 1980.
- (22) Dupin, H.; McCarty, P. *Environ. Sci. Technol.* **1999**, *33*, 1230–1236.
- (23) APHA; AWWA; WPCF. *Standard methods for the examination of water and wastewater*, 16th ed.; Franson, M. A. H., Ed.; American Public Health Association: Washington, DC, 1985; p 1268.
- (24) Koplik, J. J. *Physics C: Solid State Phys.* **1981**, *14*, 4821–4837.
- (25) Kirkpatrick, S. *Rev. Modern Phys.* **1973**, *45*, 574–588.
- (26) Dupin, H. J. Ph.D. Thesis, Department of Civil and Environmental Engineering, Stanford University, Stanford, CA, 1999.
- (27) Taylor, S. W.; Milly, P. C. D.; Jaffe, P. R. *Wat. Resour. Res.* **1990**, *26*, 2161–2169.
- (28) *Primitive sensory and communication systems: the taxes and tropisms of microorganisms and cells*; Carlile, M. J., Ed.; Academic Press: London, New York, 1975; p 258.
- (29) Witt, M. E.; Dybas, M. J.; Worden, R. M.; Criddle, C. S. *Environ. Sci. Technol.* **1999**, *33*, 2958–2964.

Received for review April 22, 1999. Revised manuscript received January 3, 2000. Accepted January 5, 2000.

ES990452F